

Assimilation of Ice Concentration in an Ice–Ocean Model

R. W. LINDSAY AND J. ZHANG

Polar Science Center, Applied Physics Laboratory, University of Washington, Seattle, Washington

(Manuscript received 14 October 2004, in final form 27 June 2005)

ABSTRACT

Ice concentration is a critical parameter of the polar marine environment because of the large effect sea ice has on the surface albedo and heat exchange between the atmosphere and the ocean. Simulations of the energy exchange processes in models would benefit if the ice concentration were represented more accurately. Reanalysis simulations that use historical wind and temperature fields may develop erroneous ice concentration estimates; these can be corrected by using observed ice concentration fields. The ice concentration assimilation presented here is a new method based on nudging the model ice concentration toward the observed concentration in a manner that emphasizes the ice extent and minimizes the effect of observational errors in the interior of the pack. The nudging weight is a nonlinear function of the difference between the model and the observed ice concentration. The simulated ice extent is improved with the assimilation of ice concentration but is not identical to the observed extent. The simulated ice draft is compared to that measured by upward-looking sonars on submarines and moorings. Significant improvements in the ice draft comparisons are obtained with assimilation of ice concentration alone and even more with assimilation of both ice concentration and ice velocity observations.

1. Introduction

A major method for understanding the state of the Arctic marine environment and how it is changing is to perform reanalyses of the system over the historical period of record using coupled ice–ocean models. The model used here is forced with surface pressure and temperature fields that are closely linked to observations so that the simulated ice thickness and concentration is a reasonably faithful recreation of the actual fields. The simulated ice thickness can then be used to determine the major modes of variability of the ice thickness and the physical processes that are important in their formation.

The simulations from the model alone suffer from several sources of error: parameterizations of physical processes, limitations of temporal and spatial resolution, and uncertainties in the forcing fields. These errors in the reanalysis may be reduced through assimilation of data directly related to the true state of the system. The two parameters in the Arctic marine envi-

ronment most frequently and widely observed both at the surface and from space are the ice extent and ice velocity. In addition, ice thickness is now also estimated from space with a variety of methods (Yu and Lindsay 2003; Laxon et al. 2003; Kwok et al. 2004) and may eventually be a candidate for data assimilation.

The ice extent has been reported in ship observations at selected locations for centuries, while ice extent and ice concentration observations from satellites date back to 1973 (for a history of satellite observations, see Gloersen et al. 1992). The ice concentration measured by satellites is subject to errors (Kwok 2002), particularly during the summer when extensive melt ponds on the surface of the ice are easily confused with open water in the passive microwave signals. There is more confidence in the satellite record of ice extent (the area of ice with concentrations greater than 0.15). Hence, we focus on assimilating ice concentration in a method that emphasizes the ice extent.

The ice velocity has been routinely measured from the daily changes in the locations of manned ice stations since the drift of the *Fram* (1893–96), but abundant ice drift data began with the inception of the International Arctic Buoy Program (IABP) in 1979. Typically, 10–20 buoy trajectories are now available to determine the ice drift velocity. In addition, the drift of the pack ice can

Corresponding author address: Ronald W. Lindsay, Polar Science Center, Applied Physics Laboratory, University of Washington, 1013 NE 40th Street, Seattle, WA 98105.
E-mail: lindsay@apl.washington.edu

be determined by comparing satellite images of the surface taken at different times (Filly and Rothrock 1987; Emery et al. 1991). The satellite sensors can be passive microwave, active microwave (radar), thermal, or visible. The satellite measurements have extensive spatial coverage and differing temporal resolution and coverage. We have previously reported our methods for assimilating ice velocity (Zhang et al. 2003), and focus in this study on the assimilation of ice concentration.

This paper is organized as follows: the model is described in section 2; the data assimilation methods are presented in section 3; comparisons with observed ice draft measurements are made in section 4; and comments and conclusions are found in section 5.

2. Model description

Our coupled ice–ocean model that has been used in a wide variety of studies. The ice model is a multcategory ice thickness and enthalpy distribution model with the following five main components: 1) a momentum equation that determines ice motion, 2) a viscous-plastic ice rheology with an elliptical yield curve that determines the relationship between ice deformation and internal stress, 3) a heat equation that determines ice temperature and ice growth or decay, 4) two ice thickness distribution equations for deformed and undeformed ice that conserve ice mass, and 5) an enthalpy distribution equation that conserves ice thermal energy. The first two components are described in detail by Hibler (1979). The ice momentum equation is solved using the Zhang and Hibler (1997) numerical method for ice dynamics. The heat equation is solved, over each category, using Winton's (2000) three-layer thermodynamic model, which divides the ice in each category into two layers of equal thickness beneath a layer of snow. The ice thickness distribution equations are described in detail by Flato and Hibler (1995). The ocean model is based on the Bryan–Cox model (Bryan 1969; Cox 1984), with an embedded mixed layer described by Kraus and Turner (1967). Detailed information about the ocean model is in Zhang et al. (1998).

The model domain covers the Arctic Ocean and the Barents and Greenland–Iceland–Norwegian Seas. It has a horizontal resolution of $40 \text{ km} \times 40 \text{ km}$, 21 vertical ocean levels, and 12 thickness categories each for undeformed ice, ridged ice, ice enthalpy, and snow. The ice thickness categories and bottom topography can be found in Zhang et al. (2000). The model domain is illustrated in Fig. 1 and the region of primary interest, the Arctic Ocean, is marked.

The model is forced with surface wind and temperature records from the National Centers for Environ-

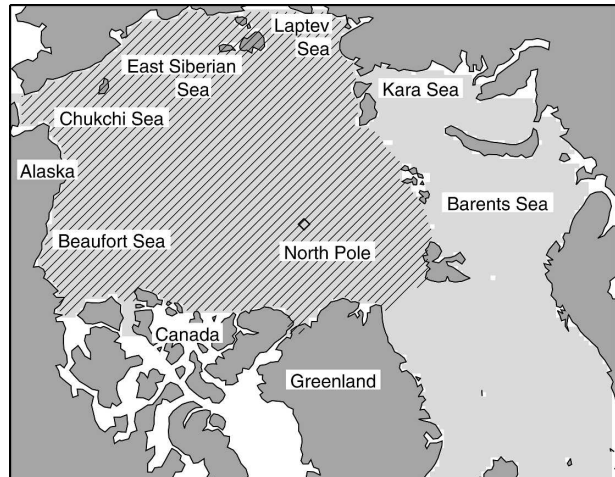


FIG. 1. The gray ocean regions depict the model domain. The cross-hatched area is the Arctic Ocean, the averaging region for the ice thickness and ice extent.

mental Prediction–National Center for Atmospheric Research (NCEP–NCAR) reanalysis (Kalnay et al. 1996). The NCEP–NCAR reanalysis is from a global atmospheric weather prediction model that assimilates all available weather data to estimate the state of the global atmosphere. Here we use only the daily averaged sea level pressure (SLP) and the 2-m air temperature fields (T2m) for the 56-yr period of 1948–2003. The specific humidity and longwave and shortwave radiative fluxes are calculated following the method described by Parkinson and Washington (1979) based on the SLP and T2m fields. Model input also includes river runoff and precipitation (Hibler and Bryan 1987; Zhang et al. 1998).

The model configuration is very similar to that of Zhang et al. (2003), but in this study we use NCEP–NCAR reanalysis T2m and SLP fields instead of those from the International Arctic Buoy Program in order to analyze a longer period. The geostrophic wind speeds from the NCEP–NCAR reanalysis SLP fields are in general greater than those from the IABP pressure fields. Over the 7-yr period of 1992–98, the geostrophic wind speed over the Arctic Ocean averaged 6.5 m s^{-1} for the IABP fields and 7.3 m s^{-1} for the reanalysis fields, which is a difference of 12%. To compensate for this change in the mean geostrophic wind speed when changing the forcing dataset, the drag coefficient in the model was adjusted to improve the correspondence between the simulated ice velocity and that measured by the buoys when no data assimilation was included. The seasonally varying drag coefficient follows that of Overland and Colony (1994), with a minimum value of 0.97×10^{-3} in the winter and a maximum of 1.42×10^{-3} in

the summer. The model was initialized with an 18-yr integration using the forcing for the years of 1948–50.

Here we use three model runs. The first includes no data assimilation, “model only,” and covers the 56-yr period of 1948–2003; the second includes data assimilation (DA) of ice concentration from the Global Sea Ice (Gice) dataset, “Gice-DA,” and covers the same time interval; the third includes assimilation of both the ice concentration and the ice velocity, “GiceV-DA,” and covers just the 25-yr period of 1979–2003 when abundant ice velocity measurements are available.

3. Data assimilation

The ice concentration is from a dataset originally created by Chapman and Walsh (1993). The dataset, called Gice, is obtained from the British Atmospheric Data Centre [BADC; information available online at <http://badc.nerc.ac.uk/data/gosta>; a more recent version is the Hadley Centre Global Sea Ice and Sea Surface Temperature (HadISST) dataset; Rayner et al. 1996]. It consists of monthly averaged ice concentration on a 1° grid. In the satellite era it is based largely on various satellite measurements, and in the presatellite era on ship reports and climatology. In particular, the data for the first 5 yr of this study, through 1952, are largely based on climatology. For 2003 only the HadISST ice concentrations are used because the Gice dataset ends in 2002. The monthly data were linearly interpolated to daily intervals.

The Gice dataset has a uniform value of 1.00 in the interior of the pack, even in the summer when many surface observations show the presence of at least some open water. The model shows summer values of 0.80–0.99, which are consistent with field observations. Because of the errors in the summer Gice dataset ice concentration in the interior of the pack (as well as errors in summer ice concentration based on passive microwave observations), assimilation of ice concentration is accomplished in a method that emphasizes the extent over the concentration. The observations are weighted heavily only when there is a large discrepancy between the model and the observed concentration. Each day the model estimate C_{mod} is nudged to a revised estimate \hat{C}_{mod} with the relationship

$$\hat{C}_{\text{mod}} = C_{\text{mod}} + K(C_{\text{obs}} - C_{\text{mod}}). \quad (1)$$

For combining two estimates of the same quantity, the optimal least squares value of the weighting K is (Deutsch 1965)

$$K = \frac{R_{\text{mod}}^2}{R_{\text{mod}}^2 + R_{\text{obs}}^2}, \quad (2)$$

where R_{mod}^2 is the error variance of the model estimate and R_{obs}^2 is the error variance of the observations. However, this expression assumes normally distributed unbiased errors, and with a bounded quantity like concentration the errors are not Gaussian and may be biased. We have limited information about the errors for either the model or the observations, except that in the interior of the pack the concentration is poorly measured compared to the variability. We believe that at the ice edge the observations have a better signal-to-noise ratio, and if there is a discrepancy between the model and the observations, the observations should be weighted heavily. The weighting factor used here is

$$K = \frac{|C_{\text{obs}} - C_{\text{mod}}|^\alpha}{|C_{\text{obs}} - C_{\text{mod}}|^\alpha + R_{\text{obs}}^2}, \quad (3)$$

where C_{obs} is the observed concentration, R_{obs}^2 is the error variance of the observations, and the exponent $\alpha = 6$ (an expression recommended by D. Thomas 1998, personal communication). This large exponent means that only if the difference between the observations and the model is large are the observations heavily weighted, in effect only assimilating the ice extent. If the error variance of the observations is small, the gain approaches 1. We use a fixed value of $R_{\text{obs}} = 0.05$. However, the error variance of the Gice dataset ice concentration is not well known and must vary considerably, both with time or location and with the ice concentration. In the interior of the pack in the winter it may be low while in the marginal ice zone or in the summer it may be higher. A better understanding of the errors in the observations would help the data assimilation procedures considerably. Using this fixed value of R we tried different values of α . We found that if α is too small (observations are heavily weighted for smaller differences) numerical instabilities develop in the ocean model. If α is large, the simulation is less tightly constrained to match the observations. Figure 2 shows the shape of the weighting factor K for three different values of α and shows that if the difference between the model and the observed ice concentration is above 0.5 the observations are weighted heavily.

The observed ice extent in the Arctic Ocean, as represented in the Gice dataset (Fig. 3a), show that the fraction of the area that is open water ($C < 0.15$) is greatest in September when the mean is 11% of the total area. The well-known trend in the recent summer open-water extent is obvious. The minimum ice extent reported by Serreze et al. (2003) for 2002 is seen here as a year of very low ice extent, but in this analysis of just the Arctic Ocean, 2003 has an even lower extent. This is consistent with the near-record low summer ice extents seen in 2003 and 2004 (Stroeve et al. 2005). The

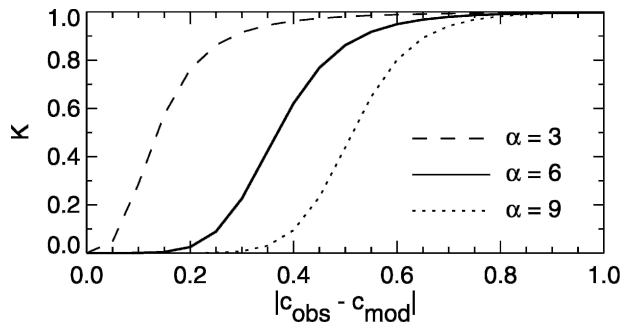


FIG. 2. The weighting factor K in the assimilation of ice concentration for three values of α . This study uses $\alpha = 6$.

difference between the observations and the model-only and Gice-DA simulations are also shown. The model-only simulation does moderately well with a mean error in September of 2% less open water, an rms difference of 4%, and a skill score of 0.67. The skill score as used here is defined as

$$S = 1 - \frac{\frac{1}{n} \sum (C_{\text{obs}} - C_{\text{mod}})^2}{\frac{1}{n} \sum (C_{\text{obs}} - \bar{C})^2}, \quad (4)$$

where the numerator of the fraction is the mean-square difference between the model and the observations and the denominator is the variance of the observations. This skill score is similar to a squared correlation coefficient except that no allowance is made for a linear fit, so it includes the effects of bias or gain errors. As expected, the differences are smaller with assimilation of the Gice data—the mean difference drops to -1% , the rms difference is 2%, and the skill score rises to 0.90. The difference is not zero because the observations are not heavily weighted when both the model and the observations show low or high ice concentrations. So, while assimilation of the ice concentrations improves the representation of ice extent in the model, the model-only simulation performs reasonably well without the benefit of the observations. This is an encouraging result, because data assimilation is not appropriate for correcting very large model errors.

Changes in the model thickness distribution were made to accommodate the change in the ice concentration in a manner that minimized changes in the ice mass by removing or adding ice to the thinnest ice classes. An alternative would be to add ice in thicker categories. For example, Lindsay (2003) describes adding ice with a thickness of 0.5 m in the summer so that it does not melt away too fast. In addition to this nudging step, it was necessary to spatially smooth the salt flux in the top ocean layer to prevent numerical instabilities in the model, instabilities that disappear only with reduced

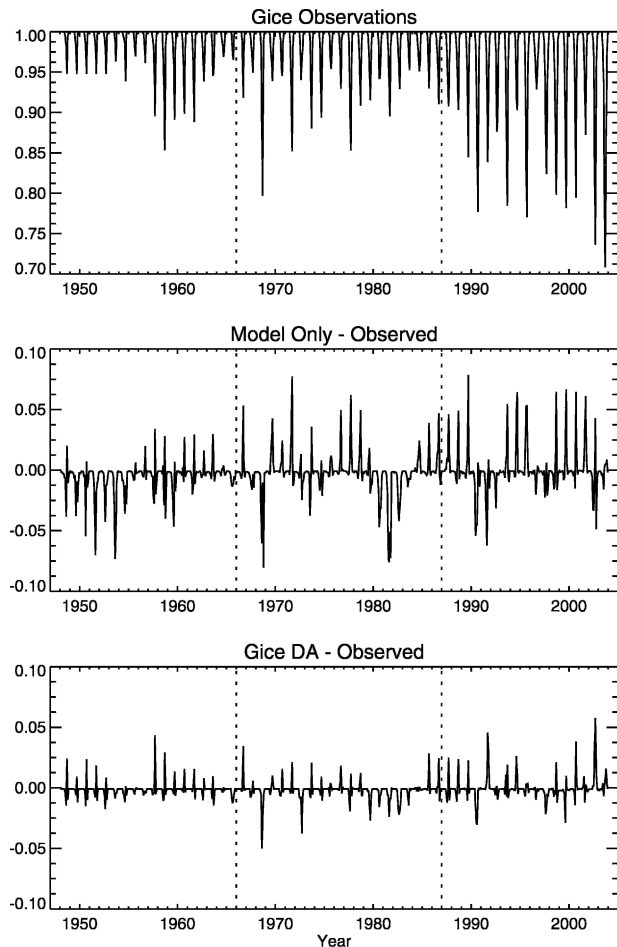


FIG. 3. Monthly mean ice extent in the Arctic Ocean determined as the area with ice concentration greater than 0.15 and expressed as a fraction of the area of the Arctic Ocean. (top) The Gice (observed) dataset, (middle) the difference between the model-only simulation and the observed extent, and (bottom) the difference between the Gice-DA simulation and the observed extent. The lines at 1966 and 1987 mark the times of local maxima in the basinwide mean ice thickness.

model time steps. The smoother used is the classic nine-point kernel with weights $(1, 2, 1; 2, 4, 2; 1, 2, 1)/16$. This large salt flux occurred occasionally when there was a persistent mismatch between the open water in the Gice dataset and the air temperature field, which, if the temperature was very low, produced very rapid refreezing of the model open water when data are assimilated. The differences in the salinity fields between the cases with and without assimilation of the ice concentration are small, with mean differences less than 1 psu at the surface, where the differences are largest. These changes in the salt flux represent a class of problems that are symptomatic of data assimilation schemes that use replacement or nudging for one of the prognostic variables. The change is in violation of the physical

processes represented in the model, and an increase in the quality of one of the variables may come at the cost of decreased quality of another, in this case the salt flux.

The ice velocity measurements are assimilated with an optimal interpolation scheme outlined in Zhang et al. (2003). We use velocity measurements from both buoy- and Special Sensor Microwave Imager (SSM/I)-derived ice displacement measurements. The buoy velocities were obtained from the IABP, and SSM/I 85-GHz ice displacement measurements were provided by the Jet Propulsion Laboratory Polar Remote Sensing Group. The buoy velocities are 24-h averages and the SSM/I velocities are based on 2-day displacements. The passive microwave displacement estimates are based on a maximum correlation method applied to sequential images of the ice cover (Kwok et al. 1998). While the SSM/I estimates have a substantially larger error standard deviation than the buoys (0.057 versus 0.007 m s^{-1} ; Lindsay 2002), their large number and excellent spatial coverage make them a valuable addition to the present analysis.

The ice velocity and ice concentration are assimilated in the GiceV-DA simulation, which begins in 1979. In the time series of the mean ice speed averaged over the area of the Arctic Ocean (Fig. 4), the model-only and Gice-DA simulations do a very good job of reproducing the basinwide mean ice speed compared to that of the GiceV-DA simulation. The deformation rates from the three simulations (not shown) are also quite similar.

The time series of the basinwide mean ice thickness for all three simulations is shown in Fig. 5. The vertical lines mark the occurrence of the two prominent maxima in the ice thickness. The Gice-DA simulation averages at 0.25 m thinner than the model-only simulation. The assimilation of ice concentration reduces the basinwide mean thickness primarily by reducing the thickness in the marginal seas. The thinning in the marginal seas is seen in Fig. 6, which shows the difference between the Gice-DA simulation and the model-only simulation for the period of 1979–2003. This thinning of

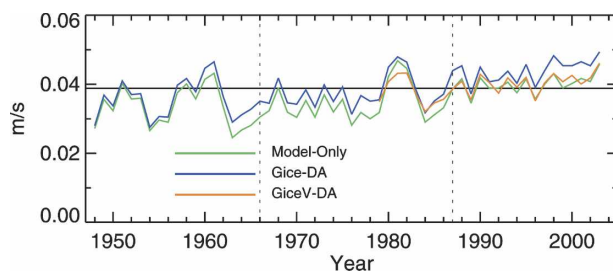


FIG. 4. Annual mean ice speed averaged over the Arctic Ocean from the three simulations. The black line indicates the mean value for the Gice-DA simulation.

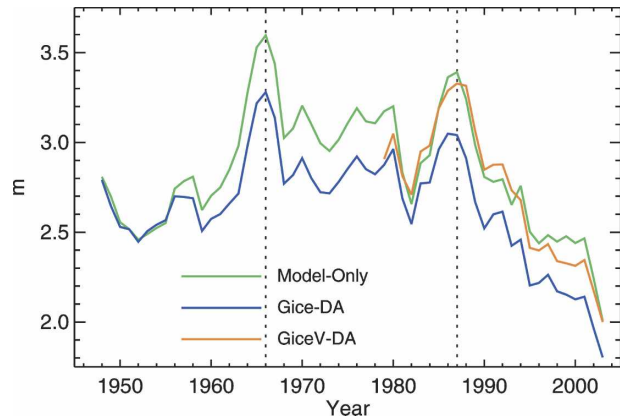


FIG. 5. Time series of the annual mean ice thickness in the Arctic Ocean from all three simulations. The vertical lines mark the years of the two prominent maxima in the ice thickness and are used as reference points in other figures.

the ice in the marginal seas after assimilation of ice concentration is likely because of the method in which the thickness distribution is modified to accommodate the change in the concentration mandated by Eq. (1). If the model ice concentration is too large, ice is removed from the distribution even if the thinnest ice is quite thick, while if ice is added to the distribution, it is added only to the 0.1-m ice thickness bin. This asymmetric addition and removal of ice leads to a thinning of the mean ice thickness. The assimilation of ice velocity in the GiceV-DA simulation thickens the ice again, primarily in the Beaufort Gyre on the Pacific side of the central basin, so that it is very similar, in the mean, to that of the model-only simulation. This thickening is accomplished primarily through modification in the mean advection of the ice pack when ice velocity measurements are assimilated, not to changes in the deformation rates.

4. Observed and modeled ice draft comparisons

Validation of the simulated ice thickness is performed with measurements of the ice draft from sub-

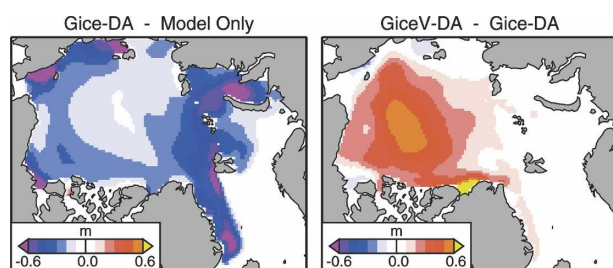


FIG. 6. Differences of the mean ice thickness from the model-only simulation and the Gice-DA simulation, and the Gice-DA simulation and the GiceV-DA simulation.

marines and moored upward-looking sonar (ULS). The submarine measurements were obtained from the National Snow and Ice Data Center (NSIDC) Submarine Upward Looking Sonar Ice Draft Profile Data and Statistics dataset. It includes eight cruises conducted under sea ice by the U.S. Navy as part of the Scientific Ice Expeditions (SCICEX) program between 1987 and 1997. These data were recorded digitally by the Digital Ice Profiling System (DIPS) II with a narrow beam sonar (approximately 3°). These submarine data were also compared in detail to the current model by Rothrock et al. (2003, hereafter RZY03) and Zhang et al. (2003). Here we repeat some of the analysis in order to document the performance of the current configuration of the model. The important differences in the configuration are that here it is forced with NCEP–NCAR reanalysis winds and temperatures instead of IABP winds and temperatures, and here it also incorporates data assimilation procedures.

In addition to the submarine cruises, we use moored ULS measurements from the Fram Strait obtained by the Norsk Polar Institute. Summaries of the comparisons for each of our three model runs and from each of the datasets are shown in Table 1. The mean ice drafts measured by submarines are for track lengths of 50 km, and the model mean ice thickness is taken from the simulations at the corresponding times and locations with no smoothing.

The comparisons with the submarine data improve when ice concentration is assimilated, then improve again when both ice concentration and velocity are assimilated. Assimilation of ice concentration increases the thickness bias but improves the rms difference and the correlation. As mentioned above, the method of modifying the thickness distribution may contribute to this thinning. The map of the difference between the model-only and GiceV-DA simulations (Fig. 6) indi-

cates that the difference is least in the interior of the basin—the region most heavily sampled in the submarine measurements. Hence, the mean difference between the two simulations shown in the table (-0.19 m) is much less than that shown for the whole basin (Fig. 5). The GiceV-DA simulation has the smallest bias, the smallest rms difference, and the largest correlation coefficient. The assimilation of ice concentration and velocity also increased the skill over that of the model-only simulation. The ice draft skill scores of the three simulations are 0.20 for the model only, 0.31 for Gice-DA, and 0.49 for GiceV-DA. The standard deviation of the ice draft indicates that the model variability in the ice thickness is too small in all three simulations. This is likely because the resolution of the model and forcing fields is inadequate to retrieve the full spatial variability of the ice thickness field that is measured by the submarines.

Figure 7 shows the difference between the observed and model ice draft for the GiceV-DA simulation. The plots for the other two simulations are very similar, including the spatial distribution of the differences, although the correlations are smaller. The first panel shows the locations of the comparisons and the difference between the model and the simulated ice draft. The pattern is very similar to that shown by RZY03, with the model showing ice that is too thick on the Pacific side of the basin and too thin on the Atlantic side. This pattern is further illustrated with Fig. 7c, where the difference between the model and the observations is plotted versus the x component of the loca-

TABLE 1. Model ice draft compared to observed ice draft.

	N	Mean (m)	Bias (m)	Std dev (m)	Rms diff (m)	Correlation (R)
Submarines, 1987–97						
Observed	835	2.35		1.06		
Model only	835	2.24	-0.11	0.78	0.95	0.51
Gice-DA	835	2.05	-0.30	0.72	0.88	0.63
GiceV-DA	835	2.33	-0.02	0.75	0.76	0.70
Fram Strait, 1990–99						
Observed	188	2.47		0.87		
Model only	188	2.21	-0.27	0.60	0.94	0.29
Gice-DA	188	1.83	-0.64	0.65	1.06	0.41
GiceV-DA	188	2.01	-0.47	0.62	0.91	0.49

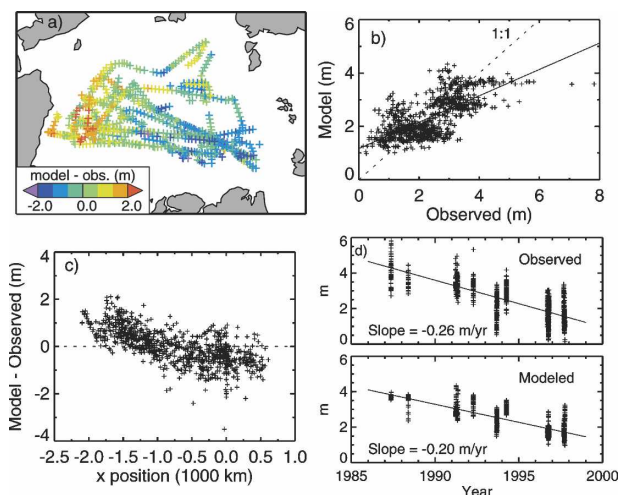


FIG. 7. Comparisons of the GiceV-DA simulation ice drafts and the submarine ice draft measurements: (a) locations of the comparisons (the color gives model – observed), (b) the model draft vs the measured draft, (c) the difference vs the x component (horizontal map component) of the locations, and (d) the observed and modeled values vs the dates of the observations.

tion (horizontal axis in the map). The trend across the basin is very consistent. In the model-only and Gice-DA simulations the trend of the difference across the basin is even larger. Figure 7b shows that the model ice is too thick when the observations show thin ice and too thin when the observations show thick ice. The correlation is 0.70. If all of the observations are combined in yearly averages, the correlation increases to 0.97, indicating that the interannual variability is well captured even if the spatial patterns are less well so. Both the observations and the model show declining trends in the ice draft over time, as seen in RZY03. The trend over time of the observed and modeled ice draft for this selection of points is shown in Fig. 7d. The model underestimates the trend in the thickness for these times and locations.

The spatial pattern of the model bias is puzzling because it persists even when ice velocity measurements are assimilated and the mean advective patterns are well estimated. One possibility is that there may be some large-scale error in the thermodynamic processes, either in the forcing or in the model physics. Possibly the assumption of spatially uniform cloud cover is in error, and by accounting for spatial variability in the clouds the bias can be reduced. Other possibilities are that the deformation rates are incorrect, even after assimilation of ice velocity, leading to incorrect ridging, or that the ice redistribution estimated in consequence of the deformation is wrong.

The Fram Strait ULS data come from a series of moorings deployed by the Norsk Polar Institute and the Alfred Wegener Institute between 1990 and 1999 (the work is ongoing). The moorings were deployed in the vicinity of 78.2° – 78.8° N and 3.4° – 7.0° W. The Fram Strait comparisons indicate that in all three model runs the simulated ice thickness is too thin, and the variability is again too small compared to the observations. This is consistent with the spatial pattern seen in the difference between the submarine ice draft measurements and the model in Fig. 7c. The correlation improves with assimilation of ice concentration and even more with ice velocity, but it remains quite low compared to that found with the submarines. Unlike with the submarine measurements, the mooring data are from near the same location so that only temporal variability is included in the signal and little spatial variability is measured. The skill scores for all three simulations are negative because the rms differences are less than the observed standard deviation.

These validation studies show that while the model has some significant problems in reproducing the thickness field at the largest scales accurately, the skill of the model is still very significant. The downward trend in

the observed ice drafts (-0.23 m yr^{-1}) is also well represented in the model, though it is not as large (-0.16 m yr^{-1} for the GiceV-DA simulation).

5. Comments and conclusions

A new method to assimilate ice concentration that emphasizes the ice extent has been introduced. The method uses a nudging technique in which the weighting is a strong function of the difference between the model and the observed ice concentration. The assimilated ice concentration improves the match with the observed extent, but the match is not identical. The assimilation of ice concentration most greatly affects the thickness of the ice in the marginal ice zones, thinning the mean ice thickness by more than 0.5 m in some locations. Our method of adjusting the thickness distribution to accommodate for the changes in the open-water area (minimizing changes in the ice mass) leads to a bias in the adjustments in that more ice mass is removed when the open-water area is increased than is added when the open-water area is reduced.

Changes in both the ice mass and the salt flux in the model illustrate that some fields in the model will no longer be in strict adherence to the physical principles of the model when data assimilation is accomplished through nudging. Another aspect of the assimilation schemes described here is that the velocity and concentration are assimilated independently from independent datasets and so they may not be physically consistent with each other or with the thermodynamic forcing fields. Ideally, the assimilation scheme would maintain the physical principles embodied in the model.

The assimilation of ice concentration significantly improves the match of the model ice draft with the measured draft. The Gice assimilation improves the correlation of ice draft over the model-only simulation both for the submarine measurements and for the Fram Strait moored measurements. The best correspondence between the simulated and the measured ice draft is with the assimilation of both the ice concentration and ice velocity. The assimilation of the ice concentration thins the ice, most strongly in the marginal ice zones. The trend in ice draft in the period of 1986–99 is less in the model simulations than is observed in the submarine measurements where model estimates and measurements are matched in time and space. A significant bias still exists in the large-scale ice thickness pattern, even with the assimilation of ice velocity measurements. The assimilation of ice concentration may also negatively impact the salt flux in some limited areas because of the artificial removal of ice and the subsequent refreezing of the model ocean.

The assimilation of ice concentration in a coupled ice–ocean model improves the representation of ice extent in the model simulations and thereby improves the representation of the surface energy balance in the marginal ice zones. It is a simple way to ensure that reanalysis of the historical evolution of the polar marine system is more faithful to the actual conditions observed.

Acknowledgments. The buoy ice velocity data were obtained from the International Arctic Buoy Program, the SSM/I ice velocity data were obtained from the Radar Remote Sensing Group at the Jet Propulsion Laboratory, the submarine ice draft data were obtained from the National Snow and Ice Data Center, and the NCEP–NCAR reanalysis data were obtained from the National Center for Atmospheric Research. The Gice and HadISST datasets were obtained from the British Atmospheric Data Center. We gratefully acknowledge discussions with M. Steele, D. Rothrock, and A. Schweiger, and the helpful comments of the reviewers. This work was supported by the NASA Office of Cryospheric Sciences Program, the NOAA Arctic Research Program, and the NSF Arctic Natural Sciences Program.

REFERENCES

- Bryan, K., 1969: A numerical method for the study of the circulation of the world oceans. *J. Comput. Phys.*, **4**, 347–376.
- Chapman, W. L., and J. E. Walsh, 1993: Recent variations of sea ice and air temperatures in high latitude. *Bull. Amer. Meteor. Soc.*, **74**, 33–47.
- Cox, M. D., 1984: A primitive equation, three-dimensional model of the oceans. GFDL Tech. Rep. 1, NOAA/Geophysical Fluid Dynamics Laboratory, 143 pp.
- Deutsch, R., 1965: *Estimation Theory*. Prentice-Hall, 269 pp.
- Emery, W. J., C. W. Fowler, J. Hawkins, and R. H. Preller, 1991: Fram Strait image-derived ice motions. *J. Geophys. Res.*, **96**, 4751–4768.
- Filly, M., and D. A. Rothrock, 1987: Sea ice tracking by nested correlations. *IEEE Trans. Geosci. Remote Sens.*, **GE-25**, 570–580.
- Flato, G. M., and W. D. Hibler III, 1995: Ridging and strength in modeling the thickness distribution of Arctic sea ice. *J. Geophys. Res.*, **100** (C9), 18 611–18 626.
- Gloersen, P., W. J. Campbell, D. J. Cavalieri, J. C. Comiso, C. L. Parkinson, and H. J. Zwally, 1992: *Arctic and Antarctic Sea Ice, 1978–1987, Satellite Passive Microwave Observations and Analysis*. National Aeronautics and Space Administration, Special Publication 511, 290 pp.
- Hibler, W. D., III, 1979: A dynamic thermodynamic sea ice model. *J. Phys. Oceanogr.*, **9**, 817–846.
- , and K. Bryan, 1987: A diagnostic ice–ocean model. *J. Phys. Oceanogr.*, **17**, 987–1015.
- Kalnay, E., and Coauthors, 1996: The NCEP/NCAR 40-Year Reanalysis Project. *Bull. Amer. Meteor. Soc.*, **77**, 437–471.
- Kraus, E. B., and J. S. Turner, 1967: A one-dimensional model of the seasonal thermocline: II. The general theory and its consequences. *Tellus*, **19**, 98–106.
- Kwok, R., 2002: Sea ice concentration from passive microwave radiometry and openings from SAR ice motion. *Geophys. Res. Lett.*, **29**, 1311, doi:10.1029/2002GL014787.
- , A. Schweiger, D. A. Rothrock, S. Pang, and C. Kottmeier, 1998: Sea ice motion from satellite passive microwave imagery assessed with ERS SAR and buoy motions. *J. Geophys. Res.*, **103** (C4), 8191–8214.
- , H. J. Zwally, and D. H. Yi, 2004: ICESat observations of Arctic sea ice: A first look. *Geophys. Res. Lett.*, **31**, L16401, doi:10.1029/2004GL020309.
- Laxon, S., N. Peacock, and D. Smith, 2003: High interannual variability of sea ice in the Arctic region. *Nature*, **425**, 947–950.
- Lindsay, R. W., 2002: Ice deformation near sheba. *J. Geophys. Res.*, **107**, 8042, doi:10.1029/2000JC000445.
- , 2003: Changes in the modeled ice thickness distribution near the Surface Heat Budget of the Arctic Ocean (SHEBA) drifting ice camp. *J. Geophys. Res.*, **108**, 3194, doi:10.1029/2001JC000805.
- Overland, J. E., and R. L. Colony, 1994: Geostrophic drag coefficients for the central Arctic derived from Soviet drifting station data. *Tellus*, **46A**, 75–85.
- Parkinson, C. L., and W. M. Washington, 1979: A large scale numerical model of sea ice. *J. Geophys. Res.*, **84**, 311–337.
- Rayner, N. A., E. B. Horton, D. E. Parker, C. K. Folland, and R. B. Hackett, 1996: Version 2.2 of the global sea-ice and sea surface temperature data set, 1903–1994. Hadley Centre for Climate Prediction and Research Climate Research Tech. Note 74, 21 pp.
- Rothrock, D. A., J. Zhang, and Y. Yu, 2003: The arctic ice thickness anomaly of the 1990s: A consistent view from observations and models. *J. Geophys. Res.*, **108**, 3083, doi:10.1029/2001JC001208.
- Serreze, M. C., and Coauthors, 2003: A record minimum arctic sea ice extent and area in 2002. *Geophys. Res. Lett.*, **30**, 1110, doi:10.1029/2002GL016406.
- Stroeve, J. C., M. C. Serreze, F. Fetterer, T. Arbetter, W. Meier, J. Maslanik, and K. Knowles, 2005: Tracking the Arctic's shrinking ice cover: Another extreme September minimum in 2004. *Geophys. Res. Lett.*, **32**, L04501, doi:10.1029/2004GL021810.
- Winton, M., 2000: A reformulated three-layer sea ice model. *J. Atmos. Oceanic Technol.*, **17**, 525–531.
- Yu, Y., and R. W. Lindsay, 2003: Comparison of thin ice thickness distributions derived from RADARSAT Geophysical Processor System and advanced very high resolution radiometer data sets. *J. Geophys. Res.*, **108**, 3387, doi:10.1029/2002JC001319.
- Zhang, J., and W. D. Hibler, 1997: On an efficient numerical method for modeling sea ice dynamics. *J. Geophys. Res.*, **102**, 8691–8702.
- , W. D. Hibler III, M. Steele, and D. A. Rothrock, 1998: Arctic ice–ocean modeling with and without climate restoring. *J. Phys. Oceanogr.*, **28**, 191–217.
- , D. A. Rothrock, and M. Steele, 2000: Recent changes in Arctic sea ice: The interplay between ice dynamics and thermodynamics. *J. Climate*, **13**, 3099–3114.
- , D. Thomas, D. A. Rothrock, R. W. Lindsay, Y. Yu, and R. Kwok, 2003: Assimilation of ice motion observations and comparisons with submarine ice thickness data. *J. Geophys. Res.*, **108**, 3170, doi:10.1029/2001JC001041.